

Dark Matter as a Guide Toward a Light Gluino at the LHC

Daniel Feldman^a, Gordon Kane^a, Ran Lu^a, and Brent D. Nelson^b

^a*Michigan Center for Theoretical Physics,
University of Michigan, Ann Arbor, MI 48109, USA*

^b*Northeastern University, Dept. of Physics, Boston, MA, 02115, USA*

Abstract

Motivated by specific connections to dark matter signatures, we study the prospects of observing the presence of a relatively light gluino whose mass is in the range $\sim (500 - 900)$ GeV with a wino-like lightest supersymmetric particle with mass in the range of $\sim (170 - 210)$ GeV. The light gaugino spectra studied here is generally different from other models, and in particular those with a wino dominated LSP, in that here the gluinos can be significantly lighter. The positron excess reported by the PAMELA satellite data is accounted for by annihilations of the wino LSP and their relic abundance can generally be brought near the WMAP constraints due to the late decay of a modulus field re-populating the density of relic dark matter. We also mention the recent FERMI photon constraints on annihilating dark matter in this class of models and implications for direct detection experiments including CDMS and XENON. We study these signatures in models of supersymmetry with non-minimal soft breaking terms derived from both string compactifications and related supergravity models which generally lead to non-universal gaugino masses. At the LHC, large event rates from the three-body decays of the gluino in certain parts of the parameter space are found to give rise to early discovery prospects for the gaugino sector. Excess events at the 5 sigma level can arise with luminosity as low as $O(100)$ pb⁻¹ at a center of mass energy of 10 TeV and $\lesssim O(1)$ fb⁻¹ at $\sqrt{s} = 7$ TeV.

1. Introduction

Production of superpartners at the Large Hadron Collider (LHC), the event rates observed in the recent cosmic ray data [1, 2], and potentially in dark matter direct detection experiments [3], all may be linked to the composition of dark matter. A well motivated class of candidate models that can be tested on all of these fronts arises when the dark matter is the lightest R-parity odd supersymmetric particle (LSP) and has a substantial wino component.

However, even if the LSP is produced at the LHC at a relatively light mass, a discoverable signal at the LHC may be difficult unless colored superpartners such as the gluino, are light. There are few top down models which generically imply an LSP that is dominantly wino with a light gluino. The breaking of supersymmetry (SUSY) through a pure anomaly mediated contribution does predict an LSP that is a wino, but needs an extension to provide a consistent model. String frameworks of interest which give rise to a light gluino and predict a wino LSP include those based on the fluxless sector of G_2 compactifications from which a realistic model of soft SUSY breaking has been constructed [4]. Related models of soft breaking based on the heterotic string can also yield a light gluino with a wino-like LSP [5, 6], and a light gluino/wino-like LSP system can also arise from gaugino mass non-universality in D-brane models of soft SUSY breaking [7].

That a wino-like LSP is consistent with the PAMELA satellite data with a mass of order 200 GeV has been emphasized [8, 9, 10, 11], and recent works have begun to study the implications of a light wino with a correspondingly light gluino

[11, 12]. Generally, for a pure wino, or wino-like dark matter candidate, the predictions on the relic abundance can be in the vicinity of the WMAP data [13]. Relatively light wino-like dark matter can produce the correct relic density and have a thermal history provided it contains non-negligible bino and Higgsino components in extended theories [11], while the pure wino can do so in a non-thermal paradigm due to the decay of heavy moduli [14, 15] (for recent related work see [16, 17, 18]). The heavy moduli can add large additional post freeze-out entropy to the primordial particle density from the moduli decay into the SUSY sector. This decay also leads to a release of winos which annihilate at a temperature much lower than freeze-out.

For the class of models we are interested in here, the gluino mass is rather light, as dictated by the soft breaking of supersymmetry and electroweak symmetry breaking, leading to large gluino production cross sections with subsequent decays of the gluinos via three-body decay chains. Thus a prominent LHC signal arises from multijet production. Some early SUSY discovery prospects in multijets at the LHC over a broad class of models have been given in [19][20] (for reviews see [21],[22]).

Distinctively, here we emphasize well motivated models that yield dark matter annihilation cross sections consistent with the recent PAMELA data, and also lead to a spectrum with a light gluino. The associated production of gluinos and a wino-like LSP lead to a simultaneous probe of supersymmetry at colliders and in present dark matter experiments, where the gluino is linked to the chargino and neutralino through its dominant three body decay channels. The analysis of electroweak gauginos at colliders with mass degeneracy between the LSP and chargino

has been studied in great detail (for early work see [23] and for a recent analysis see [24]) where the soft decays of the chargino can lead to a wino LSP and a charged pion, giving rise to a displaced vertex of a track length of a few centimeters.

The organization of this paper is as follows: In Section 2 we briefly review a soft breaking sector of interest which gives rise to a light wino and a light gluino and serves to illustrate the effects of the expected high jet multiplicity from the production of gluinos at the LHC. We then discuss the numerical simulations that allow us to make contact between the theory and the data and enable a connection between the predictions for the LHC and to possible signals of dark matter. Following this, in Section 3 we analyze the early discovery prospects of such models at the LHC for benchmark models and also for a large collection of models. The above is all carried out in the framework of the G_2 models with a pure wino LSP and a light gluino.

In Section 4 we examine a larger class of models in the context of relic density and direct and indirect detection of dark matter. We include models which deviate from a pure wino, but still have a substantial wino component. Here, as before, the soft breaking of supersymmetry and radiative electroweak symmetry breaking dictate the mass of relatively light gluino in the models of interest. We optimistically conclude in Section 5.

2. Soft Breaking with Tree and Anomalous Contributions

2.1. General Framework

The underlying framework we work in is described by $\mathcal{N} = 1$ supergravity. We first consider the G_2 – MSSM [4] which has a generalized sector of soft SUSY breaking derived from both [25] a tree level supergravity contribution and an anomalous contribution.¹ The soft parameters can be parametrized at the unification scale as $m_0 = s \cdot m_{3/2}$, $M_a = f_a \cdot m_{3/2}$, $A_3 = a_3 \cdot m_{3/2}$ where $m_{3/2} \sim \mathcal{O}(10 - 100)$ TeV is the gravitino mass, m_0 is a universal scalar mass, M_a are the gaugino masses, and A_3 are the tri-linear couplings of the third generation. Here the parameters (s, f_a, a_3) are functions of the microscopic theory which are determined entirely from the effective supergravity model. The soft parameters are well approximated by (for the complete analytical expressions see [4]) $s \sim 1$, $f_a = f'_a \alpha_G - \epsilon \eta$, where $f'_{1,2,3} = (0.35, 0.58, 0.64)$, and $\eta = 1 - \alpha_G \delta$ parametrizes gauge coupling corrections in the tree level sector of the gaugino masses. The parameter $\epsilon \sim (0.02 - 0.03)$ arises as a consequence of the hidden sector potential which is responsible for tuning the cosmological constant to zero. The terms entering for the tri-linears of the third generation are well approximated by $a_3 \sim (3/2)m_{3/2}$ up to small corrections in the normalized Yukawas and the normalized volume V_7 of the G_2 manifold, the latter of which enters in the determination of the gravitino mass. The ratio of the Higgs vacuum expectation values is generically in the range $\tan\beta \sim 1.5 - 2.0$ as μ and B are both taken to arise from the quadratic term in the Kahler potential, and are similar in magnitude. Here the largeness of the gravitino mass

decouples the scalars while the gaugino masses are suppressed relative to the gravitino mass, where the suppression enters via the volume of hidden sector three cycles. The physical values of the soft parameters are sensitive to the precise value of the unified gauge coupling and threshold corrections. The largeness of the gravitino mass generically drives the μ term to be order $m_{3/2}$ for electroweak symmetry breaking, which in turn induces a relatively large self energy correction [28] to the electroweak gaugino masses [4].

The models studied in reference [4] did not have a solution of the μ problem, but simply assumed that μ and the associated soft breaking term $B\mu$ arose from the quadratic term in the Kahler potential. When the issues of embedding the Standard Model in the G_2 manifold are fully understood it could happen that μ is small by symmetry arguments, e.g. U(1) charges force the bilinear term to vanish. Then if μ was of the same order as M_2 there would be some higgsino mixture in the G_2 wino, so the theories would have a wino-like LSP instead of a pure wino one. In this paper we use “ G_2 ” to refer to the pure wino case of reference [4]. If the theory developed to imply a wino-like LSP the results for describing the PAMELA data and LHC predictions would change very little; however predictions on dark matter direct detection would be considerably modified.

2.2. Analysis

In this work we have implemented the complete analytical expressions for soft breaking terms of the G_2 -MSSM into SOFTSUSY[29]. The analysis includes the gaugino mass threshold corrections [28] with 2 loop scalar corrections, 2-loop RGEs for the Higgs and gaugino masses, μ , and Yukawa and gauge couplings [27, 29]. Branching fractions have been computed with SUSYHIT [30] and production of signal and backgrounds are generated with PYTHIA [31] and PGS [32] with the level 1 (L1) triggers designed to efficiently reproduce CMS specifications [35] (for detailed discussions see e.g. [33]). Signal and background have been simulated at $\sqrt{s} = (7, 10, 14)$ TeV in order to generalize our predictions for preliminary LHC runs and future operational center of mass energies. Specifically, SM backgrounds have been generated with QCD multi-jet production due to light quark flavors, heavy flavor jets ($b\bar{b}$, $t\bar{t}$), Drell-Yan, single Z/W production in association with quarks and gluons (Z + jets / W + jets), and ZZ , WZ , WW pair production resulting in multi-leptonic backgrounds. Laboriously, samples were generated at $\sqrt{s} = (7, 10, 14)$ TeV with up to 5 fb^{-1} of luminosity. In PGS4 jets are defined through a cluster-based algorithm which has a heavy flavor tagging efficiency based on the parametrizations of the CDF Run II tight/loose (secondary) vertex b-tagging algorithm [34]. The standard criteria for the discovery limit of new signals is that the SUSY signals should exceed either $5\sqrt{N_{\text{SM}}}$ or 10 whichever is larger, i.e., $N_{\text{SUSY}}^c > \text{Max}\{5\sqrt{N_{\text{SM}}^c}, 10\}$, where c indicates the channel of interest.

The signature space of the models we probe has distinctive dark matter predictions. The models we consider are dominated by dark matter annihilations into W^+W^- and can yield a significant flux of cosmic antimatter in the galactic halo (for early

¹Models dominated by a tree level contribution to the soft terms are also considered in Section 4.

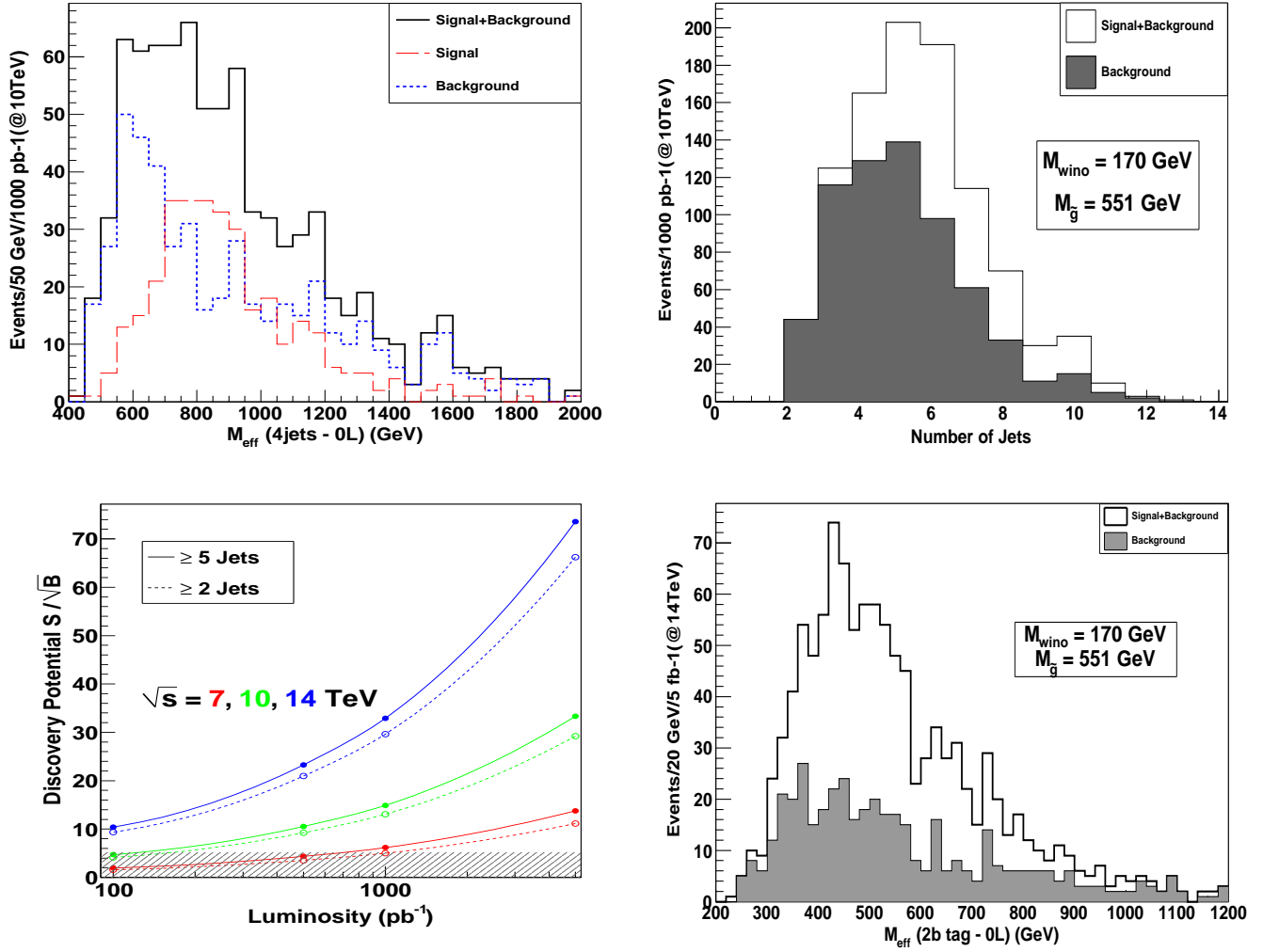


Figure 1: (Color online) Upper left panel: $M_{eff}^{4jets} = \sum_{J=1-4} P_T^J(J) + P_T^{miss}$ at 10 TeV with 1 fb^{-1} for the G_2^1 model benchmark with $S_T \geq 0.25$ (transverse sphericity), $P_T^{miss} \geq 200 \text{ GeV}$ and a lepton veto. The backgrounds mainly comes from dijets, $t\bar{t}$ and W + jets. Upper right panel: Distribution of jet number showing excesses in events with large jet multiplicities at low luminosity. Lower left panel: Discovery reach for the same model with $\sqrt{s} = (7, 10, 14) \text{ TeV}$. Lower right panel: Same model and cuts as the upper panel for 14 TeV with 5 fb^{-1} in the variable $M_{eff}^{2b} = \sum_{J=1-2} P_T^b(J) + P_T^{miss}$.

work see [38, 39, 40, 41]). The annihilation cross section receives an enhancement relative to other SUSY modes since it is s-wave and has a relative strength dictated by the SU(2) gauge coupling and the wino component of the LSP. The models are made consistent with the relic density constraints as will be discussed. For the analysis of dark matter annihilation cross sections and their resultant fluxes we employ fragmentation functions from DarkSUSY [36] using PYTHIA. In this work we also model cosmic fluxes with GALPROP v50.1p [37].

3. Early Discovery Prospects and Concrete Signatures

In theories with wino LSPs, the dominant LHC production modes are not strictly those from strongly produced SUSY. The production modes of the wino (\tilde{N}_1) and the lightest chargino (\tilde{C}_1) are competitive with the gluino (\tilde{g}) production and fre-

quently are larger. However due to the small splittings (a fraction of a GeV) between the wino and chargino the decay products here are soft. Except for larger gluino masses, we find that most events that pass the triggers do indeed come from $\tilde{g}\tilde{g}$ production, though as much as 30% of the events come from electroweak production. Thus the dominant production modes are $pp \rightarrow [(\tilde{g}\tilde{g}), (\tilde{N}_1\tilde{C}_1), (\tilde{C}_1^\pm, \tilde{C}_1^\mp)]$. The decays modes lead to rich jet and missing energy signatures with a sizeable number of leptons in the final state. In particular the dominant decays are as follows: $\tilde{g} \rightarrow [(\tilde{N}_2 t\bar{t}), (\tilde{N}_1 b\bar{b}), (\tilde{N}_1 q\bar{q}), (\tilde{C}_1^\pm b t + \text{h.c.}), (\tilde{C}_1^\pm d u + \text{h.c.})]$ with secondary decays $\tilde{N}_2 \rightarrow \tilde{C}_1 W^* \rightarrow (\tilde{C}_1 l\nu_l), (\tilde{C}_1 q\bar{q}')$ and $\tilde{C}_1 \rightarrow \tilde{N}_1 W^* \rightarrow (\tilde{N}_1 l\nu_l), (\tilde{N}_1 q\bar{q}')$ with tertiary branchings of the produced standard model particles $t \rightarrow Wb$ and $W \rightarrow [(q\bar{q}'), (l\nu_l)]$.

The models are rather predictive as they typically require no more than 2-3 branchings to complete SUSY cascades resulting

Table 1: Benchmark models predicting a light gluino and a LSP that is a wino with a degenerate chargino with a light second neutralino (which is mostly bino). The last four columns carry units of GeV.

G_2^m	$m_{3/2}$ (TeV)	δ	V_7	$\tan\beta$	$m_{\tilde{g}}$	m_W	$m_{\tilde{C}_1^\pm}$	$m_{\tilde{N}_2}$
G_2^1	38.950	-2.9	30.0	1.98	551	170.2	170.4	260
G_2^2	21.186	-10.0	33.0	1.41	717	173.4	174.0	190
G_2^3	20.700	-9.3	36.0	1.57	652	176.0	176.5	185
G_2^4	20.618	-9.1	30.0	1.71	632	180.9	181.3	185
G_2^5	35.492	-5.4	32.0	1.54	761	190.5	190.6	263

Table 2: Dominant branching ratios of the gluinos.

$Br(\tilde{g} \rightarrow X)$	G_2^1	G_2^2	G_2^3	G_2^4	G_2^5
$\tilde{g} \rightarrow b\bar{b}\tilde{N}_1$	14.2	6.4	10.2	11.3	19.5
$\tilde{g} \rightarrow q\bar{q}\tilde{N}_1$	21.0	7.4	12.6	14.6	10.0
$\tilde{g} \rightarrow t\bar{t}\tilde{N}_2$	-	47.6	21.8	14.5	14.6
$\tilde{g} \rightarrow t\bar{b}\tilde{C}^- + h.c.$	18.9	16.2	20.8	20.9	24.6
$\tilde{g} \rightarrow q_u\bar{q}_d\tilde{C}^- + h.c.$	41.5	14.6	25.2	29.0	24.9

in lepton and jet signatures. While this is a typical signature of SUSY in a generic model, it is actually a prediction of the wino branch of the G_2 model as electroweak symmetry breaking corners the viable parameter space and thus the viable signature space. The decays of $\tilde{C}_1 \rightarrow \tilde{N}_1$ and their jet and lepton by-products will be very soft yet there can be radiation of gluon from the initial or final state partons that can generate a relatively hard jet. Thus one can look for a hard monojet and n-jet events with large missing energy as an early indication of the production of supersymmetric events at the LHC. In Table (1) we illustrate some typical spectra found in the G_2 models for $m_{\tilde{N}_1} \sim (170 - 190)$ GeV (precisely in the mass range pointed to by the recent PAMELA data [see Sec.(4.2)] along with the dominant branching ratio of the gluino given in Table (2).

For the G_2 models, a central prediction is a relatively light gluino over the range of wino mass that is capable of describing the PAMELA data as is illustrated in Table (1). In Figure (1) (left upper panel) one observes that the models can produce detectable multi-jet signals even at $\sqrt{s} = 10$ TeV for $\mathcal{L} \sim 1\text{fb}^{-1}$ of integrated luminosity under the standard 5σ discovery reach criteria in the kinematic variable $M_{eff}^{A_{jets}} = \sum_{J=1-4} P_T^J(J) + P_T^{\text{miss}}$. In Figure (1) (right upper panel) we show the large number of multijet signals. The analysis shows that the model can produce a large excess in hadronic jets over the backgrounds. The large jet multiplicity arises from the three body decay of the gluinos and from jets arising from initial state radiation. We find the discovery limit is optimal for 4-5 jets with a lepton veto and large missing energy cut. The lower right panel exhibits $M_{eff}^{2b} = \sum_{J=1-2} P_T^b(J) + P_T^{\text{miss}}$ with larger luminosity. The lower left panel shows the discovery reach for the same model with $\sqrt{s} = (7, 10, 14)$ TeV and 5σ can be reached with several hundred inverse picobarns of data.

3.1. Global Analysis and Discovery Prospects of Early SUSY

Having established that the highly constrained, and therefore predictive G_2 model can give rise to detectable signals of SUSY with early LHC data (see also [42]), we now extend the analysis to a larger region of the G_2 parameter space rather than focusing on a benchmark model. We have performed a detailed scan

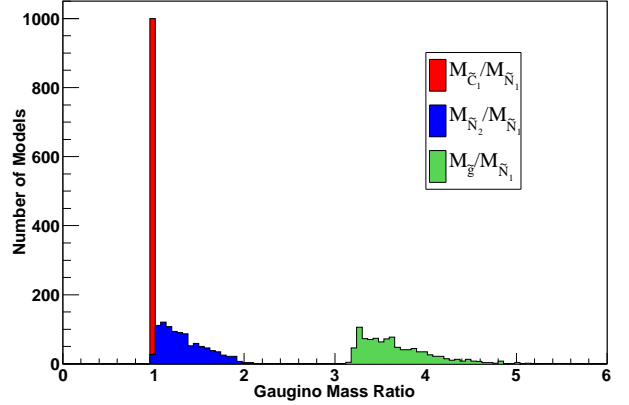


Figure 2: (Color online) Ratio of gaugino masses in the G_2 model. The predicted ratios can be quite different than those that arise in other models of soft SUSY breaking (for a comparison see Ref. [44]). The mass range here for the wino is (170 - 210) GeV and the gluino lies in the range (500-900) GeV.

of the parameter space of these models over the parameters discussed in Section 2, consistent with radiative electroweak symmetry breaking subject to the constraint that the wino mass is in the range (170 - 210) GeV. We uncover a large parameter space where the gluino can be relatively light in the G_2 model. The majority of the models have a gluino in the mass range of 500 to 900 GeV (see Fig.(2) for the corresponding gaugino mass ratios). LHC predictions with light gluino have been studied recently [43, 44, 45, 46], but without considering the connection to the PAMELA data, which we pursue in the next section.

In Table (3) we display the relatively large total theoretical production cross section before cuts (σ_{SUSY} from gluino, neutralino, chargino production) and the effective SUSY cross section σ_{eff} (cross section after the L1 triggers have been passed). One observes that the L1 triggers are well optimized for these events as a large fraction of the SUSY cross section is maintained. The substantial missing energy arises in many of the models from the prompt branching of the gluino into 2 jets and the LSP wino. Event rates at the LHC are shown in the 4-jet channel and the 2b channel with just 1fb^{-1} of integrated luminosity at $\sqrt{s} = 10$ TeV along with the ratio of the signal to the square root of the background. These models can be discovered very early with the LHC and can begin to be probed at $\sqrt{s} = 7$ TeV.

Figure (3) displays the effective SUSY production cross section after cuts (σ_{eff}) as a function of gluino mass at various center of mass energies. The (shaded) colored regions are the necessary luminosity need for a 5σ excess in steps of 200pb^{-1} of integrated luminosity where we require at least 5 jets and large missing energy ≥ 200 GeV. Thus it is apparent from the analysis that nearly all the models can produce discoverable signals with low luminosity. Remarkably, we find that with only $O(100\text{pb}^{-1})$ of data at $\sqrt{s} = 10$ TeV, the models will produce large jet-based signals which can be discovered over the SM backgrounds over a part of the parameter space, even for gluinos as light as 550 GeV with $\mathcal{L} \sim 500\text{pb}^{-1}$ at $\sqrt{s} = 7$ TeV.

Table 3: Shown is $\sigma_{\text{SUSY}}(\text{fb})$, the theoretical cross section before passing through the detector simulation, $\sigma_{\text{eff}}(\text{fb})$, the effective cross section after events have passed the L1 triggers with $\mathcal{L} = 1\text{fb}^{-1}$ at $\sqrt{s} = 10\text{ TeV}$. Observable counts in the number of tagged b-jets and multijets are also shown $N(2b)$, $N(4j)$ along with their signal to square root background ratios. The missing energy cut is $\geq 200\text{ GeV}$ and we have imposed a transverse sphericity cut of $S_T \geq 0.25$.

G_2^m	$\sigma(\tilde{g}\tilde{g})$ (fb)	$\sigma(\tilde{N}_1\tilde{C}_1)$ (fb)	$\sigma(\tilde{C}_1^+\tilde{C}_1^-)$ (fb)	σ_{SUSY} (fb)	σ_{eff} (fb)	$N(4j)$	$\frac{N}{\sqrt{B}} 4j $	$N(2b)$	$\frac{N}{\sqrt{B}} 2b $
G_2^1	1613	996	301	2910	1645	416	13.3	37	4.7
G_2^2	236	970	277	1484	353	79	2.5	22	2.8
G_2^3	481	903	280	1665	553	133	4.2	37	4.7
G_2^4	648	877	246	1773	736	217	7.0	32	4.1
G_2^5	182	696	208	1087	250	64	2.0	10	1.2

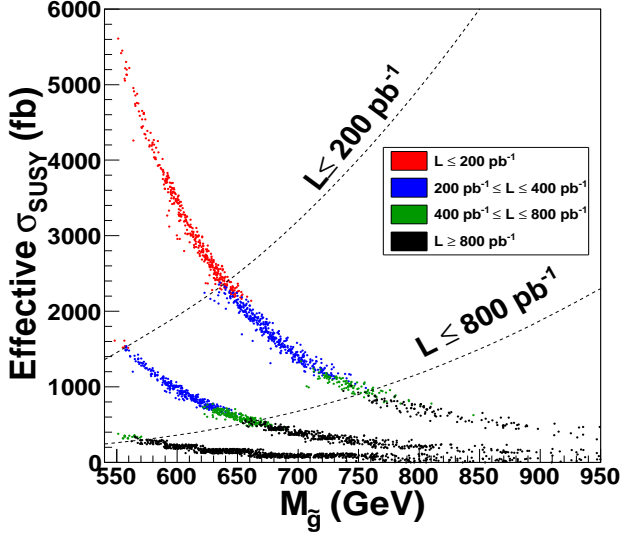


Figure 3: (Color online) Shown is the discovery potential for the gluino at low luminosity and variable LHC center of mass energy, $\sqrt{s} = (7, 10, 14)\text{ TeV}$ in terms of the effective SUSY cross section (cross section after cuts). The colored regions are the reach in steps of 200 pb^{-1} (see legend), while the approximated dashed curves are shown for the purpose of illustration. The missing energy cut is 200 GeV and $S_T \geq 0.25$. Scanning over optimal signatures, the best channels are $0L + n\text{jets}$ and $n\text{bjets}$. The analysis shows that many of the models can be discovered at $\sqrt{s} = 10\text{ TeV}$ with order 100 pb^{-1} of luminosity, and that the LHC will be able to probe a 550 GeV gluino even at $\sqrt{s} = 7\text{ TeV}$ with as little as 500 pb^{-1} of luminosity.

Models with wino-like LSPs, and thus nearly degenerate charginos and neutralinos, are well known to be difficult to study [47]. The chargino lifetime can be of order a centimeter, and the second heavier neutralino can even have order tens of GeV splitting (see Table (1) for such theory motivated examples). Once a set of gluino candidates have been identified, an off-line analysis focused towards the study of the chargino and neutralino states in the gluino decay products will be necessary.

4. General Implications of a Wino-Like LSP

In this section we relax the tight constraints of the G_2 theory space and explore the possibility of an LSP which has a significant wino component (“wino-like”), but may also have non-negligible bino and Higgsino components. One natural class of models where such an LSP is achieved are in grand

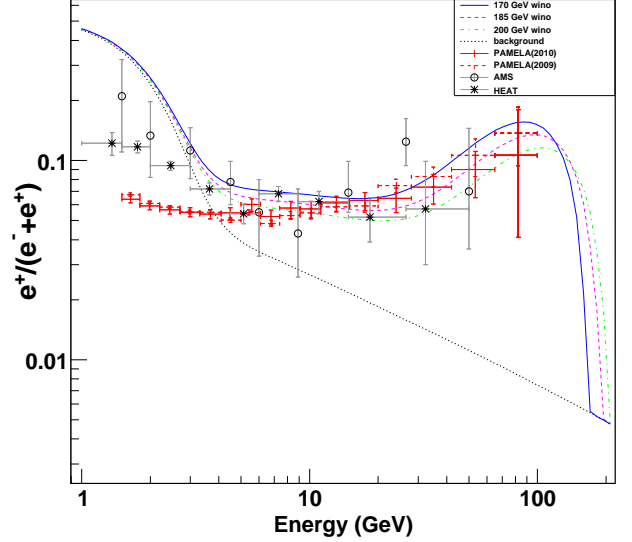


Figure 4: (Color online) Rise in the positron fraction predicted from a wino LSP with the PAMELA [1], HEAT and AMS data [55]. Different wino masses are shown to illustrate the range of masses that are well motivated to be a part of a description of the full Satellite data. Masses somewhat below 170 GeV or a bit above 200 GeV could also provide a reasonable description of the data.

unified models such as $SU(5)$, $SO(10)$, and E_6 where the GUT symmetry is broken by a non-singlet F term leading to gaugino masses at the unification scale that are non-universal, i.e., $M_a = m_{1/2}(1 + \Delta_a)$, $a = 1, 2, 3$. Such soft breaking mass terms can give rise to a wino-like LSP with a light gluino if the high scale values of the gaugino masses, M_2 and M_3 , are reduced relative to M_1 .

4.1. Relic Abundance of a Wino-Like LSP

In a general setting, the relic density can be equal to the observed one with a wino-like or pure wino LSP due to the late decay of a modulus field. Such is possible in a universe that has a non-thermal cosmological history [14]. Thus, for a single heavy modulus field Φ , in the so-called instantaneous decay approximation one obtains a reheat temperature, T_R , due to the decay Γ_Φ by assuming all energy density of Φ is transferred into radiation. The modulus decays after freeze-out and the reheat temperature is $T_R = C^{1/4} \sqrt{\overline{M}_{\text{pl}}} \Gamma_\Phi$, $C = 90/(\pi^2 g_*(T_R))$. Here $\Gamma_\Phi = c_\Phi M_\Phi^3/\Lambda^2$, $c_\Phi \sim 1$, where $\Lambda \simeq \overline{M}_{\text{pl}} \equiv \overline{M}_{\text{pl}}/\alpha$, where α parametrizes deviations from

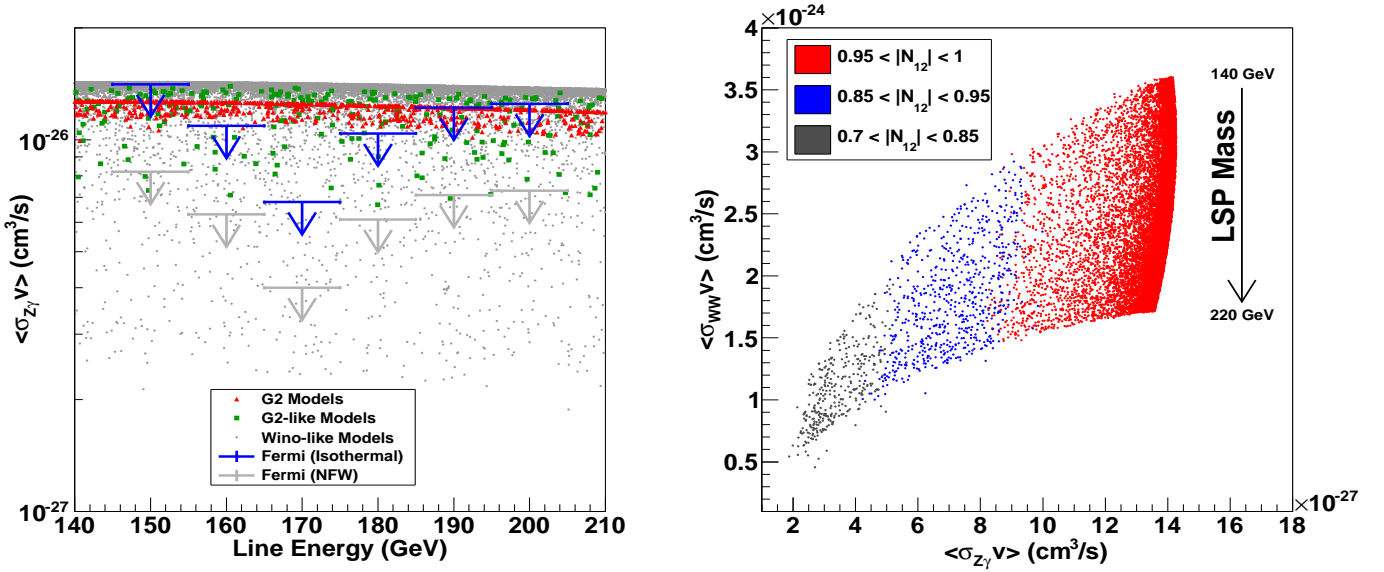


Figure 5: (Color online) Left: The models indicated by red [dark triangles] are G_2 models (pure wino and decoupled scalars) and give a good description of the PAMELA positron data. The green [dark squares] are G_2 -like models with a wino eigen-component $|N_{12}| > 0.9$ (where the normalized LSP wino component is $N_{\tilde{W}} \equiv N_{12}$), with the lightest colored superpartner being the gluino < 700 GeV but scalars can be of comparable size. Such models also describe PAMELA well. Grey [lighter points] correspond to wino-like models with wino eigen-component $|N_{12}| > 0.7$ with variable scalar and gluino masses. The upper limits are the FERMI data with either an NFW and isothermal profile assumed [70, 71, 72]. Regions which remain unconstrained by the FERMI data lie below the horizontal base of the arrows for a given profile. Right: Illustrating the strength of $\langle\sigma v\rangle$ from neutralino annihilations into WW relative to γZ and the sensitivity of the cross sections to the wino content. The mass of the LSP can be determined via $E_\gamma = M_{\text{LSP}}(1 - \delta_M)$, with $\delta_M = M_Z^2/(4M_{\text{LSP}}^2)^{-1}$. Combining the analysis of both figures shows that there is a significant region of parameter space in wino dominated models (with an accompanying light gluino) that are within reach of the FERMI data and which produce cross sections in the halo that are consistent with the PAMELA data.

the Planck scale (moduli couplings at (much lower) intermediate scales have been considered in [48, 49]). For example, $\alpha = \sqrt{V_7}$ gives $\Lambda = \overline{M}_{\text{pl}}/\sqrt{V_7} \sim (2 - 4) \times 10^{17} \text{ GeV}$ which may be interpreted as an effective string scale. Under this assumption of non-thermal (NT) production one has $\Omega_{\tilde{W}} \simeq \Omega_{\text{T}}|_{T_R}$, where $\Omega_{\text{T}}h^2$ can be computed in the usual manner (see i.e. [26]). For the s-wave dominated LSP interaction, we obtain $\Omega_{\tilde{W}}h^2 \simeq 0.32 \frac{1}{\alpha \sqrt{c_0}} (\frac{3 \times 10^{-7} \text{ GeV}^{-2}}{\langle\sigma v\rangle}) (\frac{m_{\tilde{W}}}{200 \text{ GeV}}) (\frac{m_{3/2}}{100 \text{ TeV}})^{-3/2}$, where we have used $m_\phi \lesssim 2m_{3/2}$, and where $\tilde{N}_1 \equiv \tilde{W}$. A saturation of the error corridor from the WMAP constraint on Ωh^2 is then possible for a gravitino in the mass range (40 – 60) TeV. In the G_2 models specific calculations of the relic abundance from moduli decay have been carried out [15] giving a relic density, from a string based construction, a few times larger than the experimental value unless the gravitino mass is order 100 TeV. In greater generality, the nature of soft breaking and the cosmological history of the universe may very well be closely tied together [18]. On the other hand, in a non-thermal framework one can also approach the WMAP constraint so long as T_R does not spoil BBN constraints [17].

In a thermal paradigm the relic abundance of a wino-like LSP can also be brought in accord with the WMAP data in the presence of residual Abelian gauge factors that survive down to the SUSY scale and mix weakly with the MSSM neutralinos leading to a co-annihilation enhancement [11] in an otherwise depleted relic abundance from the large annihilations of the LSP. This is to be contrasted with enhancements in the halo cross sec-

tion, i.e. through a Sommerfeld enhancement [50] or through a Breit-Wigner enhancement [51] or a boost in the flux via dark matter clumps [52, 53, 54]. Thus predictions on the relic density consistent with the production of positrons in the halo are rather model dependant, but nevertheless can account for the proper relic abundance of dark matter in such models.

4.2. Connection to the Positron Data

The data released by the PAMELA collaboration indicates a large excess in positron flux in the halo. For the case of models with MSSM field content, annihilations of the LSP into W bosons are dominant possible sources of positrons and indeed the W^+W^- production provides the needed cross section in the halo to account for the PAMELA anomaly for a pure wino [10][11] without any boost factor in the positron flux ($\langle\sigma v\rangle \sim 2.5 \times 10^{-24} \text{ cm}^3/\text{s}$). The PAMELA data can also be fit when the LSP has a non-negligible Higgsino component [11] with small boost (clump) factors in the positron flux $\sim 2 - 4$. Figure (4) illustrates fits to the data for various neutralino masses with no boost factor in the positron flux. The figure is meant to show that models with wino-like LSPs which describe the PAMELA positron ratio should have masses in the range near (170 - 200) GeV. Progress has been made towards a complete fit to both the PAMELA positron, antiproton data, and the FERMI $e^+ + e^-$ flux data using GALPROP [10] and more exhaustive analyses are currently under way. A lighter LSP could also produce the PAMELA signal with a different set

of propagation parameters. If other effects, such as small density fluctuations are included, the LSP mass range could cover slightly heavier masses.

4.3. Photon Line Spectrum and Recent Probes

The relative strength of the photon line spectrum arising from dark matter annihilations in the galaxy [56] is highly sensitive to the gaugino content of the LSP [57][58]. Thus with an essentially pure wino, as in the G_2 models, $\langle\sigma v\rangle_{\gamma Z}^{1-\text{loop}} \sim 10^{-26} \text{ cm}^3/\text{s}$, for a wino mass corresponding to the line energy of Fig.(5). Such models provide promising probes for dark matter candidates with the FERMI data [72] in the central galaxy and from dwarf galaxies. In Fig.(5) we illustrate this effect for the recently released photon data [72]. The analysis shows that annihilations of a pure wino are not inconsistent with an isothermal profile (which may be favoured by recent simulations including baryons [74]). Such a constraint is highly dependent on the profile uncertainties. At present, the PAMELA data can be described consistently with the FERMI photon data and Fig.(5) shows that FERMI is close to sensitivity needed to see a signal in the line source.

Another probe of annihilating dark matter comes from the FERMI analysis on dwarf galaxies [70, 71]. The recently reported results show the strongest constraints are from Ursa Minor and Draco implying a signal should be seen for wino masses below $\sim 300 \text{ GeV}$. This constraint assumes a NFW dwarf density profile [72] (see however [73, 74, 75]). There presently is a rather appreciable uncertainty in the predicted flux from the dwarf galaxies due in part to the integration over the density (squared) source of dark matter [76],[77]. For the case of the Draco dwarf galaxy Ref. [78] finds an uncertainty of a factor of 10 or more. A more detailed analysis will help shed light on these constraints. It would be premature to deduce that the constraints are ruling out models until the profile of the dwarf galaxies are better understood and the inclusion of more stars enters into the analyses.

4.4. CDMS and XENON

A related indication of wino-like dark matter (but not pure wino) is that of an enhanced spin independent (SI) cross section when the wino content is supplemented by non-negligible sources of Higgsino and bino content. The spin dependent cross section is also enhanced, and their contribution is not negligible, at least for Xenon based targets. For the SI interactions with admixtures of the above type one finds SI cross sections in the interesting region of $\sim O(10^{-44}) \text{ cm}^2$ [61, 62], (for recent related work see [63, 64, 65, 66, 67, 68]). For a pure wino, the tree level cross section involving the Higgs exchanges vanish and loop corrections [59] are not large enough to bring the cross section up in the region that is presently testable. Thus observation of a signal in CDMS II, XENON-100 (or EDELWEISS and other related experiments) would immediately exclude a pure wino LSP. Deviating from the pure wino by a few percent leads to a detectable (SI) cross section. For example, with soft breaking parameters $(m_0, m_{1/2}, A_0, \tan\beta, (\Delta_1, \Delta_2, \Delta_3)) = ((3000, 500, 0) \text{ GeV}, 4, (0, -.56, -0.80))$, with $\text{sign}(\mu) > 0$,

the LSP forms a *wino-like eigenstate*: $(N_{\tilde{B}}, N_{\tilde{W}}, N_{\tilde{H}_1}, N_{\tilde{H}_2}) = (0.114, -0.983, 0.127, -0.061)$, with both a large halo annihilation cross section, $\langle\sigma v\rangle_{\tilde{N}_1\tilde{N}_1 \rightarrow W^+W^-}$, and detectable SI scattering cross sections, $\sigma_{\text{SI}}(\tilde{N}_1 p)$. Specifically, one obtains the following: $\sigma_{\text{SI}}(\tilde{N}_1 p) = 1 \times 10^{-8} \text{ pb}$, and $\sigma_{\text{SD}}(\tilde{N}_1 p) = 6 \times 10^{-6} \text{ pb}$ with $\langle\sigma v\rangle_{\tilde{N}_1\tilde{N}_1 \rightarrow W^+W^-} = 2 \times 10^{-24} \text{ cm}^3/\text{s}$. Here the LSP mass is $m_{\tilde{N}_1} = 181 \text{ GeV}$ and the gluino mass is very light $m_{\tilde{g}} = 357 \text{ GeV}$. Such a model would produce discoverable jet signatures immediately at the LHC. Thus, this class of model produces positrons in the halo which describe the PAMELA data, and produces a spin independent scattering cross section within reach of the CDMS and XENON experiments (see: [60] and [66] for a similar emphasis). On the other hand if XENON-100 sees no signal, and the PAMELA data turns over at higher energies, a pure wino remains a possible and well-motivated interpretation.

5. Conclusion

In this letter we have studied collider and dark matter implications within the setting of soft supersymmetry breaking based on string compactifications and in related models with non minimal gaugino sectors. The implications of a pure wino and a wino-like LSP in association with the production of light gluinos at the LHC, along with a possible interpretation of dark matter annihilations as a cause for the rising positron ratio in PAMELA satellite data, all provide exciting possibilities for the early discovery of supersymmetry. Such a discovery will have strong implications for the underlying theory and for the nature of soft supersymmetry breaking, as well as for the cosmological history of the universe.

An underlying theory which can accommodate the positron excess, can produce testable event rates in direct detection experiments, and lead to testable signatures at the LHC due to the presence of light gluinos, all can arise with an LSP that has a substantial wino component. In addition, the wino-like LSP can have a spin independent interaction cross section that can be rather large when a non-negligible Higgsino component is present. A theory of this kind provides a compelling candidate to explain the nature of dark matter, its relic density from reheating, and its annihilations in the galaxy.

Recent photon constraints from FERMI on the above class of models are also analyzed and we have shown that there is a large region of parameter space where a wino-like LSP is consistent with the constraints. The constraints are very sensitive to the gaugino content of the wavefunction of the LSP and to the assumed halo profile. This parameter space accommodates light gluinos and therefore jets and missing energy signals that can be tested with early data at the LHC.

We have particularly emphasized, via specific models, a light gluino, and the importance of three-body decay chains which yield large jet multiplicities from the light gluino decays producing wino or wino-like LSPs. The resulting set of decays are strikingly simple and predictive with gaugino production controlling the event topologies. The nearly degenerate charginos and neutralinos arise from the three body decays of the gluino and could be identified with a careful analysis after collecting a sample of gluino events. Indeed the models discussed here are

ripe for studies at the LHC with low luminosities and at start up center of mass energies due to their large multi-jet event rates.

Acknowledgements

We collectively would like to thank Bobby Acharya, Elliot Bloom, Katherine Freese, Simona Murgia, Aaron Pierce, Jing Shao, Scott Watson and Kathryn Zurek for a broad range of discussions. This work was supported by National Science Foundation Grant PHY-0653587, and support from the Michigan Center for Theoretical Physics (MCTP) and Department of Energy grant DE-FG02-95ER40899.

References

- [1] O. Adriani *et al.* [PAMELA Collaboration], *Nature* **458**, 607 (2009); *Phys. Rev. Lett.* **102**, 051101 (2009); O. Adriani *et al.*, arXiv:1001.3522 [astro-ph.HE].
- [2] A. A. Abdo *et al.* [The Fermi LAT Collaboration], *Phys. Rev. Lett.* **102** (2009) 181101 [arXiv:0905.0025 [astro-ph.HE]].
- [3] Z. Ahmed *et al.* [CDMS Collaboration], *Phys. Rev. Lett.* **102**, 011301 (2009); J. Angle *et al.* [XENON Collaboration], *Phys. Rev. Lett.* **100**, 021303 (2008) E. Armengaud *et al.*, [The EDELWEISS Collaboration] arXiv:0912.0805 [astro-ph.CO]. Z. Ahmed *et al.* [The CDMS-II Collaboration], arXiv:0912.3592 [astro-ph.CO].
- [4] B. S. Acharya, K. Bobkov, G. L. Kane, P. Kumar and J. Shao, *Phys. Rev. D* **76**, 126010 (2007); *Phys. Rev. D* **78**, 065038 (2008); B. S. Acharya and K. Bobkov, arXiv:0810.3285 [hep-th].
- [5] G. L. Kane, J. D. Lykken, S. Mrenna, B. D. Nelson, L. T. Wang and T. T. Wang, *Phys. Rev. D* **67**, 045008 (2003); G. L. Kane, J. D. Lykken, B. D. Nelson and L. T. Wang, *Phys. Lett. B* **551**, 146 (2003).
- [6] M. K. Gaillard and B. D. Nelson, *Int. J. Mod. Phys. A* **22**, 1451 (2007).
- [7] A. Corsetti and P. Nath, *Phys. Rev. D* **64**, 125010 (2001).
- [8] P. Grajek, G. Kane, D. Phalen, A. Pierce and S. Watson, *Phys. Rev. D* **79**, 043506 (2009).
- [9] J. Hisano, M. Kawasaki, K. Kohri and K. Nakayama, *Phys. Rev. D* **79**, 063514 (2009).
- [10] G. Kane, R. Lu and S. Watson, *Phys. Lett. B* **681**, 151 (2009).
- [11] D. Feldman, Z. Liu, P. Nath, B. D. Nelson, *Phys. Rev. D* **80**, 075001 (2009); D. Feldman, arXiv:0908.3727.
- [12] B. Altunkaynak, L. L. Everett, I. W. Kim, B. D. Nelson and Y. Rao, arXiv:1001.5261 [hep-ph].
- [13] E. Komatsu *et al.* [WMAP Collaboration], *Astrophys. J. Suppl.* **180**, 330 (2009); arXiv:1001.4538 [astro-ph.CO].
- [14] T. Moroi and L. Randall, *Nucl. Phys. B* **570**, 455 (2000).
- [15] B. S. Acharya, P. Kumar, K. Bobkov, G. Kane, J. Shao and S. Watson, *JHEP* **0806**, 064 (2008).
- [16] M. Endo, K. Hamaguchi and F. Takahashi, *Phys. Rev. Lett.* **96**, 211301 (2006); S. Nakamura and M. Yamaguchi, *Phys. Lett. B* **638**, 389 (2006).
- [17] G. B. Gelmini and P. Gondolo, *Phys. Rev. D* **74**, 023510 (2006).
- [18] B. S. Acharya, G. Kane, S. Watson and P. Kumar, *Phys. Rev. D* **80**, 083529 (2009).
- [19] J. Hubisz, J. Lykken, M. Pierini and M. Spiropulu, *Phys. Rev. D* **78**, 075008 (2008).
- [20] For recent work see: L. Randall and D. Tucker-Smith, *Phys. Rev. Lett.* **101**, 221803 (2008).
- [21] G. Kane and A. Pierce, “Perspectives on LHC physics,” *World Scientific (2008)* 337 p.
- [22] P. Nath *et al.*, “The Hunt for New Physics at the Large Hadron Collider,” arXiv:1001.2693 [hep-ph].
- [23] C. H. Chen, M. Drees and J. F. Gunion, *Phys. Rev. D* **55**, 330 (1997).
- [24] M. R. Buckley, L. Randall and B. Shuve, arXiv:0909.4549 [hep-ph].
- [25] M. K. Gaillard, B. D. Nelson and Y. Y. Wu, *Phys. Lett. B* **459**, 549 (1999); J. A. Bagger, T. Moroi and E. Poppitz, *JHEP* **0004**, 009 (2000).
- [26] K. Griest and D. Seckel, *Phys. Rev. D* **43**, 3191 (1991).
- [27] S. P. Martin and M. T. Vaughn, *Phys. Rev. D* **50**, 2282 (1994).
- [28] D. M. Pierce, J. A. Bagger, K. T. Matchev and R. j. Zhang, *Nucl. Phys. B* **491**, 3 (1997).
- [29] B. Allanach, *Comput. Phys. Commun.* **143**, 305 (2002).
- [30] A. Djouadi, M. M. Muhlleitner and M. Spira, *Acta Phys. Polon. B* **38**, 635 (2007).
- [31] T. Sjostrand, S. Mrenna, P. Skands, *JHEP* **0605**, 026 (2006)
- [32] J. Conway *et al.*, PGS-4.
- [33] D. Feldman, Z. Liu and P. Nath, *Phys. Rev. Lett.* **99**, 251802 (2007); *JHEP* **0804**, 054 (2008); arXiv:0911.0217 [hep-ph], PLB in Press.
- [34] D. E. Acosta *et al.* [CDF Collaboration], *Phys. Rev. D* **71**, 052003 (2005).
- [35] G. L. Bayatian *et al.* [CMS Collaboration], *J. Phys. G* **34**, 995 (2007).
- [36] P. Gondolo, J. Edsjo, P. Ullio, L. Bergstrom, M. Schelke and E. A. Baltz, *JCAP* **0407**, 008 (2004).
- [37] A. W. Strong and I. V. Moskalenko, *Astrophys. J.* **509**, 212 (1998).
- [38] M. S. Turner and F. Wilczek, *Phys. Rev. D* **42**, 1001 (1990); M. Kamionkowski and M. S. Turner, *Phys. Rev. D* **43**, 1774 (1991); E. A. Baltz and J. Edsjo, *Phys. Rev. D* **59**, 023511 (1998); A. Bottino, F. Donato, N. Fornengo and P. Salati, *Phys. Rev. D* **58**, 123503 (1998); L. Bergstrom, J. Edsjo and P. Ullio, *Astrophys. J.* **526**, 215 (1999).
- [39] E. A. Baltz, J. Edsjo, K. Freese and P. Gondolo, *Phys. Rev. D* **65**, 063511 (2002).
- [40] G. L. Kane, L. T. Wang and J. D. Wells, *Phys. Rev. D* **65**, 057701 (2002).
- [41] J. Hisano, S. Matsumoto, O. Saito and M. Senami, *Phys. Rev. D* **73**, 055004 (2006).
- [42] S. Sekmen, Ph. D. thesis, CMS TS-2009/025.
- [43] B. S. Acharya, P. Grajek, G. L. Kane, E. Kuflik, K. Suruliz and L. T. Wang, arXiv:0901.3367 [hep-ph].
- [44] D. Feldman, Z. Liu and P. Nath *Phys. Rev. D* **80**, 015007 (2009).
- [45] S. Bhattacharya, U. Chattopadhyay, D. Choudhury, D. Das and B. Mukhopadhyaya, arXiv:0907.3428 [hep-ph].
- [46] H. Baer, V. Barger, A. Lessa and X. Tata, *JHEP* **0909**, 063 (2009); H. Baer, S. Kraml, A. Lessa and S. Sekmen, arXiv:0911.4739 [hep-ph].
- [47] See Ref. [23] and J. L. Feng, T. Moroi, L. Randall, M. Strassler and S. f. Su, *Phys. Rev. Lett.* **83**, 1731 (1999); T. Gherghetta, G. F. Giudice and J. D. Wells, *Nucl. Phys. B* **559**, 27 (1999); A. J. Barr, C. G. Lester, M. A. Parker, B. C. Allanach and P. Richardson, *JHEP* **0303**, 045 (2003); U. Chattopadhyay, D. Das, P. Konar and D. P. Roy, *Phys. Rev. D* **75**, 073014 (2007); M. Ibe, T. Moroi and T. T. Yanagida, *Phys. Lett. B* **644**, 355 (2007); S. Asai, T. Moroi and T. T. Yanagida, *Phys. Lett. B* **664**, 185 (2008).
- [48] S. Khalil, C. Munoz and E. Torrente-Lujan, *New J. Phys.* **4**, 27 (2002); M. Endo and F. Takahashi, *Phys. Rev. D* **74**, 063502 (2006).
- [49] J. P. Conlon and F. Quevedo, *JCAP* **0708**, 019 (2007).
- [50] J. Hisano, S. Matsumoto, M. M. Nojiri and O. Saito, *Phys. Rev. D* **71**, 063528 (2005); N. Arkani-Hamed, D. P. Finkbeiner, T. R. Slatyer and N. Weiner, *Phys. Rev. D* **79**, 015014 (2009).
- [51] D. Feldman, Z. Liu and P. Nath, *Phys. Rev. D* **79**, 063509 (2009); M. Ibe, H. Murayama and T. T. Yanagida, *Phys. Rev. D* **79**, 095009 (2009).
- [52] L. Bergstrom, J. Edsjo, P. Gondolo and P. Ullio, *Phys. Rev. D* **59**, 043506 (1999).
- [53] D. Hooper, J. E. Taylor and J. Silk, *Phys. Rev. D* **69**, 103509 (2004).
- [54] D. Hooper, A. Stebbins and K. M. Zurek, *Phys. Rev. D* **79**, 103513 (2009).
- [55] M. A. DuVernois *et al.*, *Astrophys. J.* **559**, 296 (2001); J. J. Beatty *et al.*, *Phys. Rev. Lett.* **93**, 241102 (2004); M. Aguilar *et al.* [AMS-01 Collaboration], *Phys. Lett. B* **646**, 145 (2007).
- [56] L. Bergstrom and P. Ullio, *Nucl. Phys. B* **504**, 27 (1997); Z. Bern, P. Gondolo and M. Perelstein, *Phys. Lett. B* **411**, 86 (1997); P. Ullio and L. Bergstrom, *Phys. Rev. D* **57**, 1962 (1998).
- [57] P. Ullio, *JHEP* **0106**, 053 (2001).
- [58] C. E. Yaguna, *Phys. Rev. D* **80**, 115002 (2009).
- [59] J. Hisano, S. Matsumoto, M. M. Nojiri and O. Saito, *Phys. Rev. D* **71**, 015007 (2005).
- [60] D. Feldman and G. Kane, “Perspectives on Supersymmetry II”; *World Scientific*, Dec. 2009.
- [61] V. Bertin, E. Nezri and J. Orloff, *JHEP* **0302**, 046 (2003).
- [62] A. Birkedal-Hansen and B. D. Nelson, *Phys. Rev. D* **67**, 095006 (2003).
- [63] D. Feldman, Z. Liu and P. Nath, *Phys. Lett. B* **662**, 190 (2008); *Phys. Rev. D* **78**, 083523 (2008).
- [64] B. Altunkaynak, M. Holmes and B. D. Nelson, *JHEP* **0810**, 013 (2008).
- [65] D. Feldman, Z. Liu and P. Nath, arXiv:0912.4217 [hep-ph].
- [66] M. Holmes and B. D. Nelson, arXiv:0912.4507 [hep-ph].
- [67] J. Hisano, K. Nakayama and M. Yamanaka, *Phys. Lett. B* **684**, 246

- (2010).
- [68] T. Cohen, D. J. Phalen and A. Pierce, arXiv:1001.3408 [hep-ph].
 - [69] A. A. Abdo, M. Ackermann and M. Ajello, arXiv:1001.4836
 - [70] C. Farnier, [FERMI LAT Collaboration], RICAP09 (Roma International Conference on Astro-Particle Physics), May 13-15, 2009.
 - [71] S. Murgia [FERMI-LAT Collaboration], 2009 Fermi Symposium 2-5 November 2009 - Washington DC.
 - [72] F. Collaboration, J. S. Bullock, M. Kaplinghat and G. D. Martinez, arXiv:1001.4531
 - [73] A. Burkert, IAU Symp. **171**, 175 (1996) [Astrophys. J. **447**, L25 (1995)].
 - [74] F. Governato *et al.*, Nature **463**, 607 (2009).
 - [75] S. Pasetto, E. K. Grebel, P. Berczik, R. Spurzem and W. Dehnen, arXiv:1002.1085 [astro-ph.CO].
 - [76] L. Bergstrom and D. Hooper, Phys. Rev. D **73**, 063510 (2006).
 - [77] L. E. Strigari, S. M. Koushiappas, J. S. Bullock and M. Kaplinghat, Phys. Rev. D **75**, 083526 (2007).
 - [78] R. Essig, N. Sehgal and L. E. Strigari, Phys. Rev. D **80**, 023506 (2009).